Spin current injection at magnetic insulator/superconductor interfaces

V. S. U. A. Vargas ⬡ * and A. R. Moura ⬡ †

Departamento de Física, Universidade Federal de Viçosa, Viçosa 36570-900, Minas Gerais, Brazil

Opposite to the common idea of a magnetic order requirement to obtain spin current propagation, materials with no magnetic ordering have also been revealed to be efficient spin conductors. In this work, we investigate the spin current injection at the interface between a magnetic insulator and a superconductor. We are mainly interested in the paramagnetic insulator/superconductor interface; however, our model also describes the ferromagnetic phase. We used the Schwinger bosonic formalism to describe the magnetic insulator, and standard BCS theory was applied to treat the superconductor layer. In the normal-metal limit, our results are in agreement with the expected ones. For example, we found the correct spin current behavior $I \approx T^{3/2}$ at low temperature. In addition, our model shows a pronounced peak in the spin current injection at temperatures close to the superconductor transition temperature due to the superconducting quasiparticle coherence. The role of magnetic fields in the spin current injection is also investigated.

I. INTRODUCTION AND MOTIVATION

Charge currents were the basis of a very large technological development in the 20th century. Even today, most commercial devices are fundamentally electronic-based ones. However, in recent years, spintronics research has taken pride of place in the scientific community. The continuous advance in miniaturization has supported the generation, manipulation, and detection of spin current in many different material classes. Basically, spin current involves effective spin transport that can be followed or not by electrical charge current. In a ferromagnetic conductor, for example, due to the electron spin polarization the current transports spin and charge at the same time. On the other hand, pure spin currents can be obtained when charge currents of opposite spins move in opposite directions, which occurs in metals with strong spin-orbit interaction, the so-called spin Hall effect [1–5]. In insulators, the spin current is driven by magnons (or spin waves in the classical formalism) and is observed in ferromagnetic [6–8], antiferromagnetic [9–14], and paramagnetic (PMI) insulators [14–16]. Temperature gradients [the spin Seebeck effect (SSE)] [17,18] as well as time-dependent ferromagnetic magnetization [spin pumping (SP)] [7,19,20] are frequently used to generate spin current in adjacent materials. The detection of spin current in conductors can be performed by the inverse spin Hall effect [21–23], where a transverse charge current provides a detectable bias voltage. In addition, when spin current is injected into (from) a magnetic insulator, the decrease (increase) in Gilbert damping is detected by measurements of the microwave radiation emitted in the ferromagnetic resonance [6,24].

Although it is usual to consider spin current injection in ferromagnetic materials, an ordered state is not really a necessary condition in spintronics. Indeed, Shiomi and Saitoh verified SP in the paramagnetic insulator La_2NiMnO_6 [25], while Wu *et al.* performed measurements of paramagnetic SSE in $DySCO_3$ and $Gd_3Ga_5O_{12}$ [gadolinium gallium garnet (GGG)] [26]. A theoretical model to describe SSE in paramagnets and antiferromagnets (both phases without a magnetization order) was developed by Yamamoto *et al.* [27]. Curiously, GGG is a well-known substrate for growing superconductor films and FM layers of yttrium iron garnet (YIG), but only recently has it been directly applied in spin transport experiments. Due to the very low exchange coupling $J_{ex} \approx 100$ mK (8.6 μeV), GGG presents a low Curie temperature transition $T_c \approx 180$ mK. Recently, Oyanagi *et al.* demonstrated the efficiency of transporting spin in a GGG slab even at temperatures several orders above T_c [15]. Amorphous YIG is a paramagnet that also presents efficient spin transport [16]. Therefore, there is much evidence for the unnecessary condition of magnetic ordering in spin current propagation.

In this work we investigate the spin current injection from a superconductor (SC) into a paramagnetic insulator. The charge current injection at superconducting interfaces has been well known since the early 1980s. Spin-polarized quasiparticles were observed in an *s*-wave superconductor due to injected spin-polarized charge current as well as spin accumulation and spin diffusion in superconducting samples [28–30]. On the other hand, spin current injection at superconducting interfaces is a more recent topic. In Ref. [31], for example, the authors determined the influence of superconductivity in spin current through measurements of the Gilbert damping in $Ni_{80}Fe_{20}$ films grown on Nb. Yao *et al.* also investigated the spin dynamics at interfaces composed of superconducting NbN films and the ferromagnetic insulator GdN [32]. Theoretical models to describe spin current injection at SC/FM interfaces can be found in Refs. [33–35]. The scenario involving a paramagnetic insulator/normal-metal (PMI/NM) junction was analyzed by Okamoto [36]. Okamoto used the Schwinger bosonic formalism to determine the spin current

*santunionivinicius@gmail.com
†antoniormoura@ufv.br

injected and spin conductivity. Here we also adopt Schwinger bosons to describe the disordered phase in terms of spinon operators that interact with quasiparticles in the SC through an *sd* interaction at the interface. Therefore, the developed model is useful for describing the spin current injection in both NM and SC phases at the interface with FM or PM insulators. We found results compatible with similar experiments and according to the special-limit cases, for example, the superconducting gapless $\Delta = 0$ phase. It is important to note that our model corrects the discrepancy in the temperature dependence of the spin current I at NM/FM interfaces found in Ref. [36] and provides the expected $I(T) \propto T^{3/2}$ behavior at low temperatures. In the PMI/SC junction we found a pronounced peak in the spin current injection due to the quasiparticle coherence. In addition, the spin conductance dependence on external magnetic fields is investigated. We verify a decreasing spin current with increasing magnetic fields due to the quasiparticle creation restraint.

II. MODEL AND METHODS

The studied model is described by the Hamiltonian $H = H_\mathrm{m} + H_\mathrm{SC} + H_\mathrm{sd}$, where the terms define the magnetic insulator, the superconductor, and the interface interaction, respectively. Both magnetic and superconductor sides are considered three-dimensional samples, but a model of thin films can be treated with minor modifications. The *sd* Hamiltonian represents an interaction at the interface between located electrons on the insulator and conduction electrons on the normal metal. In this section, we briefly review the main points of the Schwinger formalism to represent magnetic models and the microscopic BCS theory.

The magnetic insulator is given by the standard Heisenberg Hamiltonian $H_\mathrm{m} = -J \sum_{\langle ij \rangle} \vec{S}_i \cdot \vec{S}_j$, where J is a small exchange ferromagnetic coupling and the sum is taken over nearest-neighbor spins. At low temperature, spin operators are commonly treated by using the Holstein-Primakoff (HP) bosonic representation. However, HP bosons are inaccurate for representing disordered magnetic phases. A more appropriate representation is obtained through Schwinger bosons, which are applicable to both ordered and disordered phases [37,38]. The spin operators are then replaced by two kinds of bosonic operators and written as $S_i^+ = a_{i\uparrow}^\dagger a_{i\downarrow}$, $S_i^- = a_{i\downarrow}^\dagger a_{i\uparrow}$, and $S_i^z = (a_{i\uparrow}^\dagger a_{i\uparrow} - a_{i\downarrow}^\dagger a_{i\downarrow})/2$, where $a_{i\sigma}^\dagger$ ($a_{i\sigma}$) creates (annihilates) a spinon with spin $\sigma/2$ ($\sigma = 1$ stands for up spin, and $\sigma = -1$ stands for down spin). To ensure the commutation relation $[S_i^a, S_j^b] = i\delta_{ij}\epsilon_{abc} S_i^c$ is necessary to fix the number of bosons on each site through the constraint $\sum_\sigma a_{i\sigma}^\dagger a_{i\sigma} = 2S$. The Hamiltonian is then given by

$$H_\mathrm{m} = -\frac{J}{2} \sum_{\langle ij \rangle} (: \mathcal{F}_{ij}^\dagger \mathcal{F}_{ij} : -2S^2) + \sum_i \lambda_i (\mathcal{F}_{ii} - 2S)$$
$$- \frac{g\mu_B B}{2} \sum_i (a_{i\uparrow}^\dagger a_{i\uparrow} - a_{i\downarrow}^\dagger a_{i\downarrow}), \qquad (1)$$

in which we defined the bond operator $\mathcal{F}_{ij} = a_{i\uparrow}^\dagger a_{j\uparrow} + a_{i\downarrow}^\dagger a_{j\downarrow}$ and :: represents the normal ordering operator. We include a uniform magnetic field $\vec{B} = B\hat{z}$, and the constraint is implemented by a local Lagrange multiplier λ_i. The quartic

order term is decoupled by introducing an auxiliary field $F_{ij} = \langle \mathcal{F}_{ij} \rangle$ through the Hubbard-Stratonovich transform $\mathcal{F}_{ij}^\dagger \mathcal{F}_{ij} \rightarrow F_{ij}(\mathcal{F}_{ij}^\dagger + \mathcal{F}_{ij}) - F_{ij}^2$. We consider a mean-field theory and replace F_{ij} by a uniform field F. In the same way we approximate the Lagrange multiplier by a uniform parameter λ, which implies boson conservation only on average. After a space Fourier transform, we obtain the quadratic Hamiltonian

$$H_\mathrm{m} = E_0 + \sum_q [\hbar\Omega_{q\uparrow} a_{q\uparrow}^\dagger a_{q\uparrow} + \hbar\Omega_{q\downarrow} a_{q\downarrow}^\dagger a_{q\downarrow}], \qquad (2)$$

where $E_0 = 3NJ(F^2 + 2S^2)/2 - 2NS(3JF - \mu_\mathrm{m})$ is the ground-state energy and $\hbar\Omega_{q\sigma} = \hbar\omega_q - \mu_\mathrm{m} - \sigma g\mu_B B/2$. In the above equation, N is the number of magnetic sites, $\hbar\omega_q = 3JF(1 - \gamma_q)$, and $\gamma_q = (\cos q_x + \cos q_y + \cos q_z)/3$ is the square lattice structure factor. The chemical potential $\mu_\mathrm{m} = 3JF - \lambda$ was introduced to make clear the analogy between the ordered phase transition and Bose-Einstein condensation ($-\mu_\mathrm{m}$ could also be considered a gap in spectrum energy [39]). The fields F and λ are evaluated by the minimization of the free energy $F_\mathrm{m} = -\beta^{-1} \ln(\mathrm{Tr} e^{-\beta H_\mathrm{m}})$. The extremum conditions $\delta F_\mathrm{m}/\delta\lambda = 0$ and $\delta F_\mathrm{m}/\delta F = 0$ provide the self-consistent equations

$$2S = \frac{1}{N} \sum_q (n_{q\uparrow} + n_{q\downarrow}) \qquad (3)$$

and

$$F = 2S - \frac{1}{N} \sum_q \frac{\hbar\omega_q}{3JF} (n_{q\uparrow} + n_{q\downarrow}), \qquad (4)$$

where $n_{q\sigma} = (e^{\beta\hbar\Omega_{q\sigma}} - 1)^{-1}$ is the Bose-Einstein distribution. In the disordered phase $\mu_\mathrm{m} + g\mu_B B/2 < 0$, and the self-consistent equations present a nontrivial solution for F and λ. At a critical temperature we obtain $\mu_\mathrm{m} = -g\mu_B B/2$ and the up-spin boson condensate in the $q = 0$ state ($\Omega_{0\uparrow} = 0$). As well as in standard Bose-Einstein condensation, we separate the $q = 0$ term from the sum before converting it to a momentum integral to solve the equations in the ordered phase. At low temperature, the second self-consistent equation provides $F \approx 2S$. We then include a phenomenological parameter χ to consider a small correction and express $F = 2S\chi$ ($\chi = 1$ in the limit $T \rightarrow 0$). In the long-wavelength limit, χ can be determined by the deviation magnetization per site given by

$$\frac{\Delta m}{N} = S - \langle S^z \rangle \approx \left(\frac{k_B T}{4\pi J\chi S} \right)^{3/2}, \qquad (5)$$

adopting the limit $B \rightarrow 0^+$. Here and henceforth, we will use $J\chi$ as the magnetic energy scale. Using Eq. (3), we then determine the dependence of the chemical potential μ_m on temperature and magnetic field. A graphic of $\mu_\mathrm{m}(T)$ for $B = 0$ is shown in Fig. 1 (cases with finite B present similar behavior).

The superconductor is described by the well-known BCS theory [40], whose Hamiltonian is written as

$$H_\mathrm{sc} = \sum_{k\sigma} \epsilon_k c_{k\sigma}^\dagger c_{k\sigma} - g_\mathrm{eff} \sum_{kk'} c_{k\uparrow}^\dagger c_{-k\downarrow}^\dagger c_{-k'\downarrow} c_{k'\uparrow}, \qquad (6)$$

in which g_eff is the effective superconducting interaction constant. The momentum sum is done within the range $\pm\hbar\omega_\mathrm{D}$
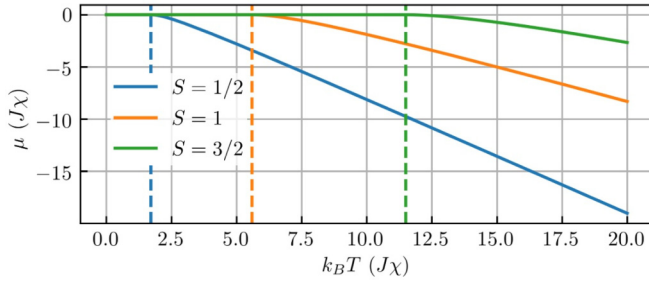
FIG. 1. The chemical potential μ_{m} as a function of temperature for $B = 0$. The vertical dashed lines represent the critical temperature of the boson condensation.

of the Fermi surface, i.e., $|\epsilon_k - \epsilon_F| < \hbar\omega_D$, where ϵ_F is the Fermi energy and ω_D is the Debye frequency. Typical energy scales for the Fermi and Debye energy are 10 and 10^{-2} eV, respectively. A population imbalance between up- and down-spin electrons is necessary to ensure spin current injection from the SC. After including the chemical potentials $\mu_\uparrow$ and $\mu_\downarrow$ for up- and down-spin electrons, respectively, the grand-canonical Hamiltonian is expressed as

$$K_{\mathrm{SC}} = C + \sum_k \Psi_k^\dagger \begin{pmatrix} \xi_k - \mu_{\mathrm{sc}} & -\Delta \\ -\bar{\Delta} & -\xi_k - \mu_{\mathrm{sc}} \end{pmatrix} \Psi_k, \qquad (7)$$

where $C = |\Delta|^2/g_{\mathrm{eff}} + \sum_k (\xi_k + \mu_{\mathrm{sc}})$ is a constant and the Nambu spinor is defined by $\Psi_k^\dagger = (c_{k\uparrow}^\dagger \quad c_{-k\downarrow})$. The quartic order interaction was decoupled by introducing the superconducting gap $\Delta = g_{\mathrm{eff}} \sum_k \langle c_{-k\downarrow} c_{k\uparrow} \rangle$. In the above equation $\xi_k = \epsilon_k - (\mu_\uparrow + \mu_\downarrow)/2$, and the SC chemical potential (the Zeeman splitting) is defined as $\mu_{\mathrm{sc}} = (g\mu_B B + \Delta\mu)/2$, with $\Delta\mu = \mu_\uparrow - \mu_\downarrow$. Here we also include the uniform magnetic field $\vec{B} = B\hat{z}$. While the superconducting ground state is composed of Cooper pairs, the excitations are given by quasiparticles (also called bogoliubons) of energy $E_k = \sqrt{\xi_k^2 + |\Delta|^2}$. The BCS Hamiltonian is diagonalized, defining new fermionic operators by the Bogoliubov transform

$$b_{k\uparrow} = \bar{u}_k c_{k\uparrow} + v_k c_{-k\downarrow}^\dagger, \qquad (8a)$$

$$b_{k\downarrow} = \bar{u}_k c_{k\downarrow} - v_k c_{-k\uparrow}^\dagger, \qquad (8b)$$

with the parameters $u_k = e^{-i\phi/2}\sqrt{(E_k + \xi_k)/2E_k}$ and $v_k = e^{i\phi/2}\sqrt{(E_k - \xi_k)/2E_k}$ (ϕ is the superconducting gap phase, $\Delta = e^{i\phi}|\Delta|$). The diagonal BCS Hamiltonian is then given by

$$K_{\mathrm{SC}} = K_0 + \sum_k (E_{k\uparrow} b_{k\uparrow}^\dagger b_{k\uparrow} + E_{k\downarrow} b_{k\downarrow}^\dagger b_{k\downarrow}), \qquad (9)$$

where $K_0 = |\Delta|^2/g_{\mathrm{eff}} + \sum_k (\xi_k - E_k)$ is a constant energy and $E_{k\sigma} = E_k - \sigma\mu_{\mathrm{sc}}$. Using the above Hamiltonian, we obtain the self-consistent gap equation

$$\Delta = \sum_k \frac{g\Delta}{4E_k}\left[\tanh\left(\frac{\beta E_{k\uparrow}}{2}\right) + \tanh\left(\frac{\beta E_{k\downarrow}}{2}\right)\right], \qquad (10)$$

which provides the result in Fig. 2. The SC temperature transition is defined as the temperature at which the gap vanishes. For $\mu_{\mathrm{sc}} > 0.707|\Delta_0|$ the SC is suppressed even at zero temperature.
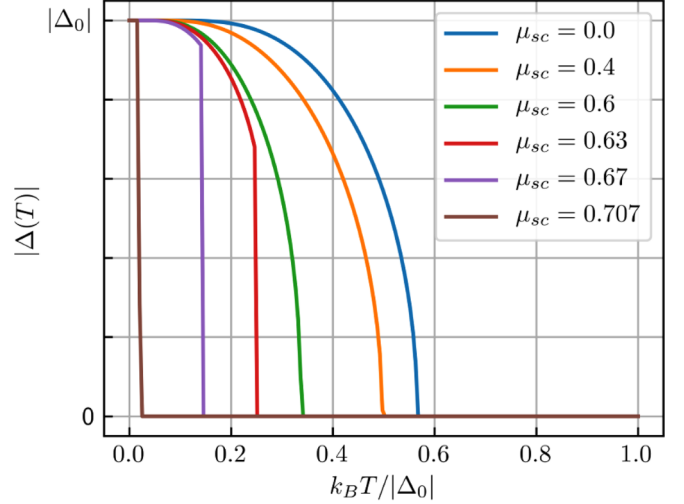

FIG. 2. The gap dependence on temperature for different values of μ_{sc}. Above the SC transition temperature the gap vanishes. For $\mu_{\mathrm{sc}} > 0.707|\Delta_0|$ the SC is suppressed even at zero temperature.

As one can see, the chemical potential difference between up- and down-spin quasiparticles favors processes with annihilation (creation) of up-spin (down-spin) quasiparticles. Therefore, a positive value of μ_{sc} provides a spin current flux from the SC into the magnetic insulator. However, the presence of polarizing terms such as the magnetic field and the chemical potential imbalance $\Delta\mu$ tend to destroy the superconducting phase [41,42]. Indeed, the gap is a decreasing function of increasing μ_{sc}, and the largest value $|\Delta_0|$ occurs when $\mu_{\mathrm{sc}} = 0$. For $\mu_{\mathrm{sc}} < 0.60|\Delta_0|$ there is a second-order phase transition, while for $0.60|\Delta_0| < \mu_{\mathrm{sc}} < 0.707|\Delta_0|$ the gap Δ presents a discontinuous jump at the NM/SC transition temperature. For $\mu_{\mathrm{sc}} > 0.707|\Delta_0|$ the superconductivity is suppressed even at zero temperature. Here we consider only the scenario where $\mu_{\mathrm{sc}} < 0.60|\Delta_0|$.

The *sd* Hamiltonian accounts for a spin-flip process at the interface at which *s*-like electrons are reflected, leading to the absorption (emission) of angular momentum from (to) the magnetic side. Since we are considering a magnetic insulator, the interface interaction does not take into account conduction electrons going into the magnetic side, and processes such as Andreev reflection are forbidden. However, the spin current injection across the interface is allowed due to the creation or annihilation of magnons (or spinon pairs of opposite spins). The interaction is expressed by

$$H_{\mathrm{sd}} = J_{\mathrm{sd}} \sum_{qkp} (S_q^- c_{k\uparrow}^\dagger c_{p\downarrow} + S_q^+ c_{p\downarrow}^\dagger c_{k\uparrow}), \qquad (11)$$

with J_{sd} being a coupling constant. Here we consider weak coupling between *s*-wave and *d*-wave electrons, so H_{sd} is treated as a small perturbation. In addition, a rough interface is assumed, which implies an independent transverse momentum sum.

III. SPIN CURRENT

We define the spin current operator as the time derivative of the difference $N_\downarrow - N_\uparrow$ of electrons close to the interface.
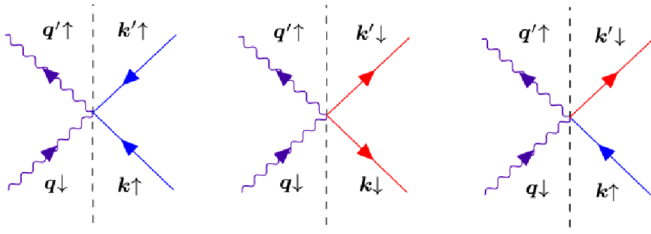
FIG. 3. The three processes describing spin current injection at the interface: annihilation (left), creation (middle), and scattering of quasiparticles (right) in the superconductor represented by the straight lines. The wavy lines represent spinons in the magnetic insulator.

Using the Heisenberg equation, we obtain $I = iJ_{sd}(V - V^\dagger)$, where the vertex operator is given by

$$V = \frac{1}{N} \sum_{qq'kk'} a_{q\downarrow}^\dagger a_{q'\uparrow} c_{k\uparrow}^\dagger c_{k'\downarrow}. \qquad (12)$$

Since we are considering the limit of weak interface interaction, the expected value $\langle I \rangle$ can be determined from the linear response theory. It is straightforward to obtain $I = \langle I \rangle = -i\hbar^{-1} \int dt\theta(t)\langle [\hat{I}(t), \hat{H}_{sd}(0)]\rangle$, where the integral extends over the entire time axis and $\theta(t)$ denotes the Heaviside step function. The caret denotes time evolution according to $H_m + H_{sc}$, and since $N_\sigma = \sum_k c_{k\sigma}^\dagger c_{k\sigma}$ commutes with the full Hamiltonian $H = H_m + H_{sc} + H_{sd}$, we can write $\hat{V}(t) = e^{i\Delta\mu t/\hbar}\tilde{V}(t)$, where the time evolution of $\tilde{V}$ is evaluated through the grand-canonical Hamiltonian. Therefore, we obtain

$$I = -\frac{2J_{sd}^2}{\hbar}\text{Im}U_{ret}(\Delta\mu), \qquad (13)$$

in which $U_{ret}(\Delta\mu)$ is the time Fourier transform of the retarded Green's function $\hbar U_{ret}(t) = -i\theta(t)\langle [\tilde{V}(t), \tilde{V}^\dagger(0)]\rangle$. As usual, the retarded Green's function is determined by the Matsubara formalism, which provides $U_{ret}(\Delta\mu)$ through the analytical continuation of $\mathcal{U}(i\omega_l) = \int \mathcal{U}(\tau)e^{i\omega_l\tau}d\tau$, where

$$\hbar\mathcal{U}(\tau) = -\langle T_\tau V(\tau)V^\dagger(0)\rangle = -\Xi_m(\tau)\Xi_e(\tau) \qquad (14)$$

is the imaginary-time Green's function. The magnetic term Ξ_m of the Green's function is given by

$$\Xi_m(\tau) = \frac{1}{N^2}\sum_{qq'}\mathcal{A}_{q\downarrow}(-\tau)\mathcal{A}_{q'\uparrow}(\tau), \qquad (15)$$

where we defined the a-operator Green's function $\mathcal{A}_{q\sigma}(\tau) = -\langle T_\tau a_{q\sigma}(\tau)a_{q\sigma}^\dagger(0)\rangle$. Equation (15) defines the annihilation of a $|q, \downarrow\rangle$ spinon state at the same time that a $|q', \uparrow\rangle$ state is created, resulting in an effective angular momentum variation of $\Delta S = \hbar$ in the magnetic insulator. Here we have assumed dissipationless spin waves. However, if necessary, a damping term can easily be implemented in the Green's function. On the other hand, the electronic part Ξ_e, written in terms of the b operators, provides

$$\begin{aligned}\Xi_e(\tau) = \sum_{kk'}[&(|u_kv_{k'}|^2 - u_kv_k\bar{u}_{k'}\bar{v}_{k'})\mathcal{B}_{k\uparrow}(-\tau)\mathcal{B}_{k'\uparrow}(-\tau)\\ &+ (|u_kv_{k'}|^2 - u_kv_k\bar{u}_{k'}\bar{v}_{k'})\mathcal{B}_{k\downarrow}(\tau)\mathcal{B}_{k'\downarrow}(\tau)\\ &+ (u_kv_k\bar{u}_{k'}\bar{v}_{k'} + \bar{u}_k\bar{v}_ku_{k'}v_{k'} + |u_ku_{k'}|^2\\ &+ |v_kv_{k'}|^2)\mathcal{B}_{k\uparrow}(-\tau)\mathcal{B}_{k'\downarrow}(\tau)], \qquad (16)\end{aligned}$$

where $\mathcal{B}_{k\sigma}(\tau) = -\langle T_\tau b_{k\sigma}(\tau)b_{k\sigma}^\dagger(0)\rangle$ is the Green's function associated with the b operators. The above equation describes three different processes that decrease the spin on the SC side by $\hbar$, resulting in an effective momentum angular transfer to the magnetic side. The first term in Eq. (16) describes the annihilation of two up-spin quasiparticles. Indeed, $\mathcal{B}_{k\uparrow}\mathcal{B}_{k'\uparrow}$ is proportional to the occupation $f_{k\uparrow}f_{k'\uparrow}$, where $f_{k\sigma} = f(E_{k\sigma})$ is the Fermi-Dirac distribution, while the multiplicative term in parentheses is the coherence factor. From Eq. (8a), the $b_{k\uparrow}$ operator gives a probability $|u_k|^2$ to annihilate an up-spin electron and $|v_k|^2$ to create a down-spin electron. Therefore, the $|u_kv_{k'}|^2$ term, for example, gives the probability of destroying a $|k, \uparrow\rangle$ electron state while a $|k', \downarrow\rangle$ electron state is created or, equivalently, a $|-k', \uparrow\rangle$ hole state is annihilated. Note that the charge is conserved in the process. In the same way, the second term represents the creation of two down-spin quasiparticles, and the last one sets the scattering of an up-spin to a down-spin quasiparticle. All processes are represented in Fig. 3.

The spin current is then composed of the sum of three terms, $I = I^a + I^c + I^s$, where the expected values I^a, I^c, and I^s are the contributions associated with annihilation, creation, and scattering of quasiparticles at the interface, respectively. The analytical continuation $i\omega_l \rightarrow \Delta\mu + i0^+$ of the quasiparticle annihilation process $\mathcal{U}^a(i\omega_l)$, for example, provides

$$\text{Im}U_{ret}^a(\Delta\mu) = \frac{\pi\hbar}{4N^2}(e^{-\beta\Delta\mu} - 1)\sum_{qq'}(1 + n_{q\downarrow})n_{q'\uparrow}\sum_{kk'}\left(1 - \frac{|\Delta|^2}{E_kE_{k'}}\right)f_{k\uparrow}f_{k'\uparrow}\delta(E_k + E_{k'} + \hbar\omega_q - \hbar\omega_{q'}). \qquad (17)$$

In general, the energy scale of $\Delta\mu$ is much smaller than the thermal energy, and we adopted $1 - e^{-\beta\Delta\mu} \approx \beta\Delta\mu$. After replacing the quasiparticle momentum sum by the continuum limit, we obtain

$$I^a(\Delta\mu) = \frac{\pi J_{sd}^2\beta\Delta\mu}{2N^2}\sum_{qq'}n_{q\downarrow}(1 + n_{q'\uparrow})\int_0^\infty dE\int_{-\infty}^0 dE'\left(1 + \frac{|\Delta|^2}{EE'}\right)f(E_\uparrow)D(E)[1 - f(E'_\downarrow)]D(E')\delta(E - E' + \hbar\omega_q - \hbar\omega_{q'}),$$

$$(18)$$

where $D(E) = \rho_F\text{Re}[(E + i\Gamma)/\sqrt{(E + i\Gamma)^2 - |\Delta|^2}]$ is the superconducting density of states endowed by the phenomenological Dynes parameter Γ and ρ_F is the normal-metal density of states at the level Fermi. Note that $D(E)$ presents two narrow peaks at $E \approx \pm|\Delta|$ and tends to unity when $|E| \gg |\Delta|$ (the normal-metal limit). The inclusion of Γ is necessary to ensure the convergence

of the energy integral. To calculate the spin current, we adopted $\Gamma = 0.05|\Delta_0|$ [43]. The I^c and I^s contributions are determined by the same procedure.

The magnetic part of the spin current requires special attention. In the ordered state, the Schwinger boson condensation takes place, and the macroscopic population term N_0 needs to be removed from the momentum sum before we adopt the continuum limit. Although we are interested in the PMI/SC junction, the spin current can also be evaluated in other situations. Therefore, we write $n_{q'\uparrow} = N_0\delta_{q,0} + n_{q'\neq 0\uparrow}$, where $N_0 \approx N$ measures the condensation of up-spinon states with $q = 0$ (the limit of weak magnetic field $B \rightarrow 0^+$ is assumed). Summing over all quasiparticle processes and separating the condensate term from the q' sum, the spin current is written as $I = I_f + I_p$, where we define

$$I_f(\Delta\mu) = \frac{N_0}{N}\frac{J_{sd}^2\beta\Delta\mu}{16\pi^2}\int_{BZ}d^3q\,n_{q\downarrow}\int_{-\infty}^{\infty}dE\left(1 + \frac{|\Delta|^2}{E(E + \hbar\omega_q - \hbar\omega_0)}\right)$$
$$\times f(E - \mu_{sc})D(E)[1 - f(E + \hbar\omega_q - \hbar\omega_0 + \mu_{sc})]D(E + \hbar\omega_q - \hbar\omega_0) \quad (19)$$

as the ferromagnetic spin current associated with the up-spinon condensation and

$$I_p(\Delta\mu) = \frac{J_{sd}^2\beta\Delta\mu}{128\pi^5}\int_{BZ}d^3q\,d^3q'\,n_{q\downarrow}(1 + n_{q'\uparrow})\int_{-\infty}^{\infty}dE\left(1 + \frac{|\Delta|^2}{E(E + \hbar\omega_q - \hbar\omega_{q'})}\right)$$
$$\times f(E - \mu_{sc})D(E)[1 - f(E + \hbar\omega_q - \hbar\omega_{q'} + \mu_{sc})]D(E + \hbar\omega_q - \hbar\omega_{q'}). \quad (20)$$

as the paramagnetic spin current. In the above equations, the momentum integration is done over the first Brillouin zone (BZ). Above the Curie temperature the condensation vanishes ($N_0 = 0$), and the spin current is only due to the paramagnetic term. In the condensate phase, below the Curie transition temperature, I_f shows an important role in the spin current behavior.

At zero temperature, the process of quasiparticle creation is the only relevant contribution to the spin current provided that $\hbar\omega_q - \hbar\omega_{q'} > 2|\Delta|$. At finite temperature, the largest spin current contributions occur when the peaks of $D(E)$ and $D(E + \hbar\omega_q - \hbar\omega_{q'})$ coincide. There are three distinct cases: (i) the quasiparticle scattering case when $\hbar\omega_q - \hbar\omega_{q'} \approx 0$, (ii) the quasiparticle creation case for $\hbar\omega_q - \hbar\omega_{q'} \approx 2|\Delta|$, and (iii) the quasiparticle annihilation case when $\hbar\omega_q - \hbar\omega_{q'} \approx -2|\Delta|$. The integrand of the spin current energy integral for $k_BT = 0.5|\Delta|$ and $\mu_{sc} = 0.01|\Delta|$ is shown in Fig. 4. The largest contribution occurs for the quasiparticle creation

process when the highest peaks of $f(E_\uparrow)D(E)$ and $[1 - f(E_\downarrow + \hbar\omega_q - \hbar\omega_{q'})]D(E + \hbar\omega_q - \hbar\omega_{q'})$ are close.

IV. RESULTS

We are mainly interested in the spin current injection at the PMI/SC interface; however, before we present the major results, to verify the model consistency we analyze other situations. As mentioned before, in the disordered phase, the ferromagnetic spin current I_f vanishes due to the absence of spinon condensation; however, at very low temperatures, I_f has an important role. Recently, Okamoto [36] determined the spin current at the magnetic/normal-metal junction in both ordered and disordered phases using the Schwinger formalism. In the limit $T \rightarrow 0$, he found a spin current dependent on T^3 instead of the known result $I \propto T^{3/2}$ [8]. Okamoto associated the different power-law behavior with the spin orientation of the injected current. However, the inclusion of the condensate contribution I_f restores the $T^{3/2}$ behavior. To see this, we consider the metal-normal limit ($\Delta = 0$) in the absence of magnetic field and the approximation

$$\int d\epsilon\, f(\xi_\uparrow)[1 - f(\xi_\downarrow)] \approx \frac{(\hbar\omega_q + \Delta\mu)e^{\beta(\hbar\omega_q + \Delta\mu)}}{e^{\beta(\hbar\omega_q + \Delta\mu)} - 1}. \quad (21)$$

Inserting the above result in Eq. (19), we obtain, for a small imbalance chemical potential,

$$I_f = \frac{N_0}{N}\frac{(\rho_F J_{sd})^2\beta\Delta\mu}{4\pi}\int_0^{\infty}dq\frac{\hbar\omega_q e^{\beta\hbar\omega_q}}{(e^{\beta\hbar\omega_q} - 1)^2}$$
$$= \frac{(\rho_F J_{sd})^2 S\beta\Delta\mu}{(J\chi S\pi)^{1/2}}(k_BT)^{3/2}, \quad (22)$$

where the long-wavelength limit $\hbar\omega_q = J\chi Sq^2$ was taken and we considered $N_0/N \approx 2S$. A similar procedure shows that $I_p \propto T^3$ due to the double Bose-Einstein distribution, and at low temperatures, we have $I \approx I_f \propto T^{3/2}$. Therefore, when the condensation term is properly considered, we recover the expected power-law dependence on T. The same result can be obtained from the Holstein-Primakoff formalism that is applicable to ordered states as well as the Schwinger
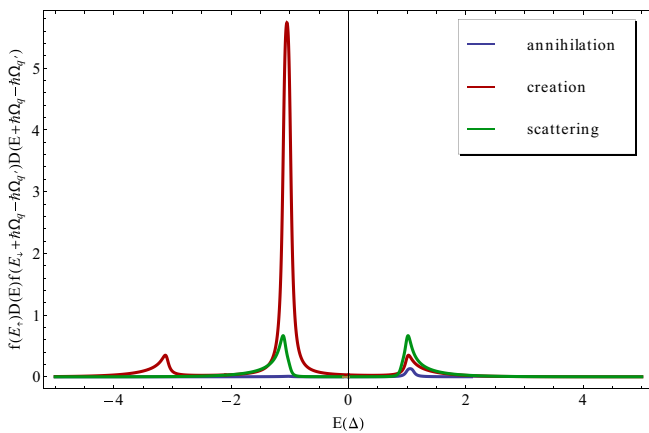

FIG. 4. The integrand of the spin current energy integral for $\hbar\omega_q - \hbar\omega_{q'} = 0.1|\Delta|$ (quasiparticle scattering process), $\hbar\omega_q - \hbar\omega_{q'} = 2.1|\Delta|$ (quasiparticle creation process), and $\hbar\omega_q - \hbar\omega_{q'} = -2.1|\Delta|$ (quasiparticle annihilation process). Here, $k_BT = 0.5|\Delta|$, and $\mu_{sc} = 0.01|\Delta|$.
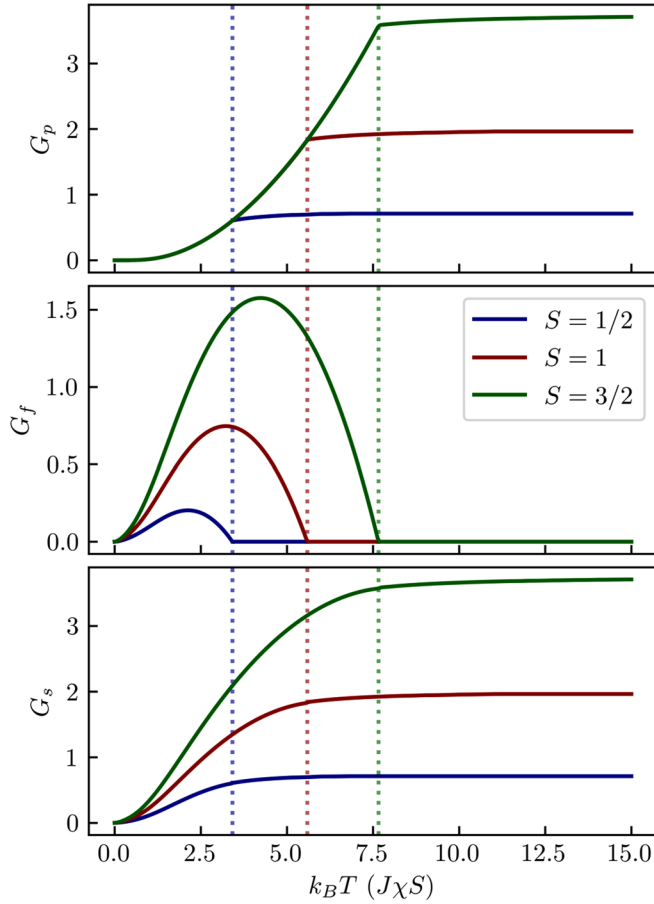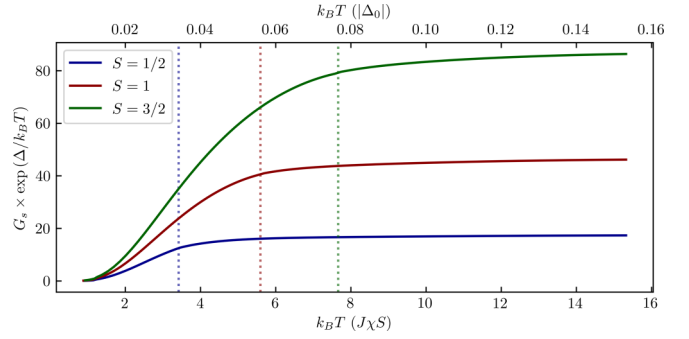
FIG. 6. The spin current injection at the FM/SC interface. Due to the superconducting gap the spin current intensity is multiplied by the Boltzmann factor $e^{-\beta|\Delta|}$ that causes a great reduction in I.

The second possible interface is the PMI/SC one. In this case we are considering temperatures on the interval $J\chi \lesssim k_B T \lesssim |\Delta_0|$ like in the GGG/NbN interface, for example. For $J\chi \ll |\Delta_0|$, the quasiparticle scattering process is the more relevant contribution to the spin current since spinons do not have sufficient energy to create or annihilate quasiparticles in the SC sample. In the paramagnetic phase, the spin current is given by Eq. (20) while $I_f = 0$. We choose $J\chi = 0.01|\Delta_0|$, and the momentum integral of Eq. (20) is taken over the energy interval $|\hbar\omega_q - \hbar\omega_{q'}| < 0.02|\Delta_0|$. The ratio G_s/G_{sat} for $B = 0$ as a function of the temperature is shown in Fig. 7. Here G_{sat} stands for the NM spin conductance when the temperature tends to the SC transition point $T = 0.568|\Delta_0|^2/k_B$ from the values above. The spin conductance presents a peak below the SC transition temperature due to the coherence factor, while G is equal to the NM spin conductance above the SC transition temperature. As one can note, above the SC transition point, the spin conductance is almost constant, and no visible variation is apparent. Our results provide the following peak values: $1.390G_{sat}$ ($S = 1/2$), $1.387G_{sat}$ ($S = 1$), and $1.384G_{sat}$ ($S = 3/2$). At very low temperatures, the magnetic ordered state occurs, and the spin conductance (as

FIG. 5. The paramagnetic (top) and ferromagnetic (center) contributions for the spin conductance for the normal metal limit and the total spin conductance (bottom). The vertical lines indicate the Curie transition temperature.

formalism in the condensate phase. In Fig. 5 we show the spin conductance G_s ($= \lim_{\Delta\mu \to 0} I/\Delta\mu$) associated with the ferromagnetic and paramagnetic spin current contribution. The result obtained from the paramagnetic spin current is identical to that presented in Ref. [36]; however, the ferromagnetic term gives a smoother transition to the flat region above the Curie transition temperature. The plateau at high temperatures is provided by the factor $k_B T$ that results from the energy integration and cancels the β multiplicative factor and the paramagnetic boson condition $n_{q\uparrow} = n_{q\downarrow}$ that hinders the spinon scattering.

Returning to the SC phase, we have two possible interfaces. The first one involves a FM/SC junction for which we adopt $J\chi \ll |\Delta_0|$. In this case, the spin current dependence on T at very low temperatures (below the Curie transition temperature) is similar to that presented in the paragraph above; however, the intensity is drastically reduced by a factor $e^{\beta|\Delta_0|}$. In the superconducting phase the probability that magnetic excitation has sufficient energy to induce spin injection is very low since $J\chi \ll |\Delta_0|$. Figure 6 shows the spin conductance behavior at low temperatures. In this limit, I is proportional to $e^{-\beta|\Delta_0|}T^{3/2}$, and when $|\Delta_0| \to 0$, we recover the result of the FM/NM junction.
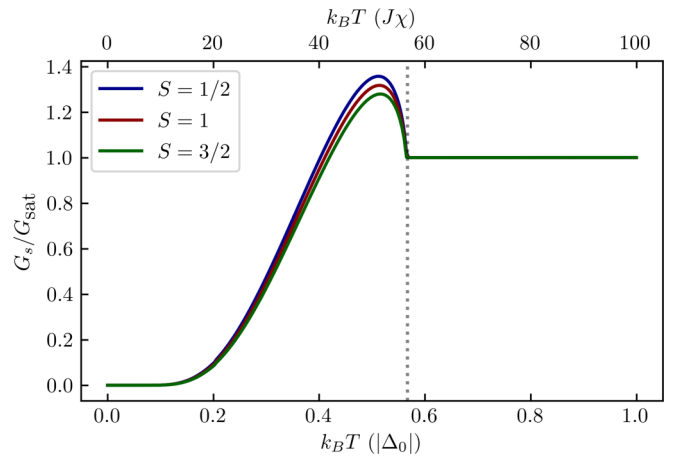

FIG. 7. The spin current injection at the PMI/SC interface. The maximum above the SC transition temperature is provided by the coherence factor.
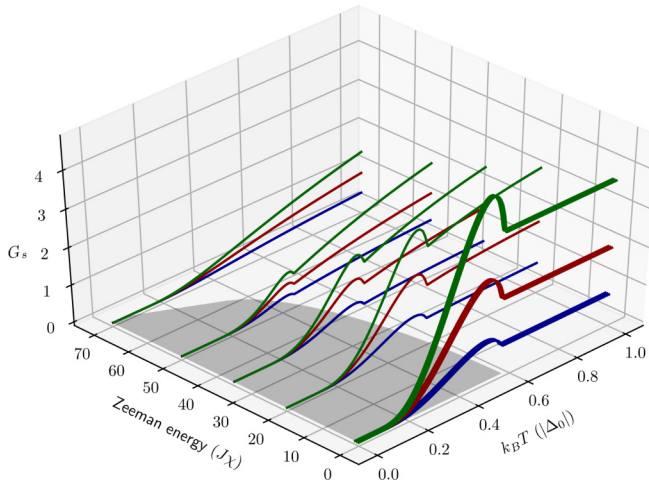
FIG. 8. The spin conductance G_s dependence on magnetic field (Zeeman energy) and temperature. The effects of small magnetic field (with Zeeman energy of the order of $J\chi = 0.01|\Delta_0|$) are negligible, while a strong magnetic field destroys the coherent behavior of the SC state. The superconductivity phase is represented by the shaded area. The blue, red, and green curves describe magnetic models with spin 1/2, 1, and 3/2, respectively.

well as the spin current) is extremely small, as analyzed in the paragraph above.

The magnetic field effect on spin conductance is shown in Fig. 8. The shaded area represents the superconductivity regime. Magnetic fields with Zeeman energy of the order of $J\chi$ have minimal effects on the spin conductance since we are adopting $J\chi = 0.01|\Delta_0|$. The curves for magnetic field with energies of 0, $0.5J\chi$, and $1J\chi$ present no visible difference. However, as is well known, high magnetic fields suppress the superconductivity, and the quasiparticle coherence is destroyed. The spin conductance for Zeeman energies larger than $0.707|\Delta_0|$ (considering $\Delta\mu = 0$) then shows the almost linear behavior $G_s \propto B$.

V. SUMMARY AND CONCLUSIONS

In this work we investigated the spin current injection at the PMI/SC interface. The usual spintronics experiments adopt

junctions with ferromagnetic layers, and only recently has the role of the disordered magnetic phase been considered. Here we used the Schwinger formalism to treat both ordered and disordered magnetic phases while the SC was described by the standard BCS theory. Therefore, we were able to identify two contributions to the spin current. The first one (here denominated as ferromagnetic spin current) is associated with the condensate part of the Schwinger bosons, while the second one (called paramagnetic spin current) is due to the bosons out of the condensate. In the limit of a vanishing SC gap, our equations provide the expected NM results with minor corrections. In a recent work, for example, Okamoto [36] used the Schwinger formalism to evaluate the spin current at the PMI/NM interface, and he found a T^3 dependence at low temperature for the spin current instead of the expected $T^{3/2}$ behavior [8]. However, in that work, the condensate contribution was not taken into account. Meanwhile, in our results, the corrected $T^{3/2}$ power law of the spin current temperature dependence was obtained due to the condensate term. However, for a temperature above the Curie transition there is no boson condensation, and the paramagnetic spin current is the only relevant contribution. For the PMI/SC junction, the spin injection occurs mainly due to scattering of bogoliubons on the SC side, while the probability of quasiparticle creation (or annihilation) processes is very low since the exchange coupling $J \ll |\Delta_0|$. Notwithstanding the lack of magnetic ordering, we showed an expressive spin current increasing at temperatures close to the SC transition. At $k_B T = 0.511|\Delta_0|$ the spin conductance shows an increase of approximately 40% when compared to the NM value due to the coherence between quasiparticles in the SC state. In addition, low magnetic fields (of the order of $J\chi \sim 0.01|\Delta_0|$) present no perceptible effect on spin conductance, while high magnetic field (larger than the critical value of $0.707|\Delta_0|/g\mu_B$) suppresses the superconductivity and reduces the spin conductance.

[1] J. E. Hirsch, Phys. Rev. Lett. **83**, 1834 (1999).

[2] S. Zhang, Phys. Rev. Lett. **85**, 393 (2000).

[3] J. Sinova, S. O. Valenzuela, J. Wunderlich, C. H. Back, and T. Jungwirth, Rev. Mod. Phys. **87**, 1213 (2015).

[4] V. P. Amin and M. D. Stiles, Phys. Rev. B **94**, 104419 (2016).

[5] V. P. Amin and M. D. Stiles, Phys. Rev. B **94**, 104420 (2016).

[6] Y. Tserkovnyak, A. Brataas, and G. E. W. Bauer, Phys. Rev. Lett. **88**, 117601 (2002).

[7] A. Azevedo, L. H. Vilela-Leão, R. L. Rodríguez-Suárez, A. F. Lacerda Santos, and S. M. Rezende, Phys. Rev. B **83**, 144402 (2011).

[8] S. Takahashi, E. Saitoh, and S. Maekawa, J. Phys.: Conf. Ser. **200**, 062030 (2010).

[9] V. Baltz, A. Manchon, M. Tsoi, T. Moriyama, T. Ono, and Y. Tserkovnyak, Rev. Mod. Phys. **90**, 015005 (2018).

[10] J. B. S. Mendes, R. O. Cunha, O. Alves Santos, P. R. T. Ribeiro, F. L. A. Machado, R. L. Rodríguez-Suárez, A. Azevedo, and S. M. Rezende, Phys. Rev. B **89**, 140406(R) (2014).

[11] S. Takei, B. I. Halperin, A. Yacoby, and Y. Tserkovnyak, Phys. Rev. B **90**, 094408 (2014).

[12] S. M. Rezende, R. L. Rodríguez-Suárez, and A. Azevedo, Phys. Rev. B **93**, 054412 (2016).

[13] L. J. Cornelissen, K. J. H. Peters, G. E. W. Bauer, R. A. Duine, and B. J. van Wees, Phys. Rev. B **94**, 014412 (2016).

[14] W. Lin, K. Chen, S. Zhang, and C. L. Chien, Phys. Rev. Lett. **116**, 186601 (2016).

[15] K. Oyanagi, S. Takahashi, L. J. Cornelissen, J. Shan, S. Daimon, T. Kikkawa, G. E. Bauer, B. J. van Wees, and E. Saitoh, Nat. Commun. **10**, 4740 (2019).

[16] D. Wesenberg, T. Liu, D. Balzar, M. Wu, and B. L. Zink, Nat. Phys. **13**, 987 (2017).

[17] H. Adachi, J.-i. Ohe, S. Takahashi, and S. Maekawa, Phys. Rev. B **83**, 094410 (2011).

[18] H. Adachi, K.-i. Uchida, E. Saitoh, and S. Maekawa, Rep. Prog. Phys. **76**, 036501 (2013).

[19] Y. Ohnuma, H. Adachi, E. Saitoh, and S. Maekawa, Phys. Rev. B **89**, 174417 (2014).

[20] A. Azevedo, L. Vilela Leao, R. Rodriguez-Suarez, A. Oliveira, and S. Rezende, J. Appl. Phys. **97**, 10C715 (2005).

[21] E. Saitoh, M. Ueda, H. Miyajima, and G. Tatara, Appl. Phys. Lett. **88**, 182509 (2006).

[22] T. Kimura, Y. Otani, T. Sato, S. Takahashi, and S. Maekawa, Phys. Rev. Lett. **98**, 156601 (2007).

[23] S. O. Valenzuela and M. Tinkham, Nature (London) **442**, 176 (2006).

[24] Y. Tserkovnyak, A. Brataas, and G. E. W. Bauer, Phys. Rev. B **66**, 224403 (2002).

[25] Y. Shiomi and E. Saitoh, Phys. Rev. Lett. **113**, 266602 (2014).

[26] S. M. Wu, J. E. Pearson, and A. Bhattacharya, Phys. Rev. Lett. **114**, 186602 (2015).

[27] Y. Yamamoto, M. Ichioka, and H. Adachi, Phys. Rev. B **100**, 064419 (2019).

[28] M. Johnson and R. H. Silsbee, Phys. Rev. Lett. **55**, 1790 (1985).

[29] M. Johnson and R. H. Silsbee, Phys. Rev. B **37**, 5326 (1988).

[30] M. Johnson, Appl. Phys. Lett. **65**, 1460 (1994).

[31] C. Bell, S. Milikisyants, M. Huber, and J. Aarts, Phys. Rev. Lett. **100**, 047002 (2008).

[32] Y. Yao, Q. Song, Y. Takamura, J. P. Cascales, W. Yuan, Y. Ma, Y. Yun, X. C. Xie, J. S. Moodera, and W. Han, Phys. Rev. B **97**, 224414 (2018).

[33] M. Inoue, M. Ichioka, and H. Adachi, Phys. Rev. B **96**, 024414 (2017).

[34] T. Kato, Y. Ohnuma, M. Matsuo, J. Rech, T. Jonckheere, and T. Martin, Phys. Rev. B **99**, 144411 (2019).

[35] V. Vargas and A. Moura, J. Magn. Magn. Mater. **494**, 165813 (2020).

[36] S. Okamoto, Phys. Rev. B **93**, 064421 (2016).

[37] D. P. Arovas and A. Auerbach, Phys. Rev. B **38**, 316 (1988).

[38] S. Sarker, C. Jayaprakash, H. R. Krishnamurthy, and M. Ma, Phys. Rev. B **40**, 5028 (1989).

[39] A. Auerbach, *Interacting Electrons and Quantum Magnetism* (Springer-Verlag, New York, 1994).

[40] M. Tinkham, *Introduction to Superconductivity*, 2nd ed. (Dover Publications, New York, 2004).

[41] G. Sarma, J. Phys. Chem. Solids **24**, 1029 (1963).

[42] M. Crisan and H. Jones, J. Low Temp. Phys. **18**, 297 (1975).

[43] M. Umeda, Y. Shiomi, T. Kikkawa, T. Niizeki, J. Lustikova, S. Takahashi, and E. Saitoh, Appl. Phys. Lett. **112**, 232601 (2018).